

# Multi-probe three-dimensional placement planning for liver cryosurgery: comparison of different optimization methods

Amir Jaberzadeh<sup>1</sup> and Caroline Essert<sup>1</sup>

<sup>1</sup> *ICUBE, Université de Strasbourg, CNRS, France*

emails: ahjaberzadeh@unistra.fr, essert@unistra.fr

## Abstract

Pre-operative planning of percutaneous thermal ablations is a difficult but decisive task for a safe and successful intervention. The purpose of our research is to assist surgeons in preparing cryoablations with an automatic pre-operative path planning algorithm able to propose a placement for multiple needles in 3D. The aim is to optimize several surgical constraints while taking into account a precise computation of the frozen area. Using an implementation of the precise estimation of the iceballs, this study focuses on the optimization in an acceptable time of multiple probes positions with 6 degrees of freedom, regarding the constraint of optimal volumetric coverage of the tumor by the combined necrosis. Pennes equation was used to solve the propagation of cold within the tissues, and included in an objective function of the optimization process. The propagation computation being time-consuming, six optimization algorithms from the literature were experimented under different conditions and compared, in order to reduce overall computation time while preserving precision. Some of them were found suitable for the conditions of our cryosurgery planning. We conclude that this combination of bioheat simulation and optimization can be appropriate for a use by practitioners in acceptable conditions of time and precision.

*Key words: Surgery planning, Derivative free optimization, Bioheat simulation*

## 1 Introduction

Minimally invasive surgery has known an increasing interest in the past decades. The small size of incisions is beneficial to patients by decreasing the discomfort as well as the time required for recovery compared to conventional surgery, all with the same benefits. Percutaneous cryoablation is a good example, in which the cancerous tissue is frozen using one or multiple needles. During this procedure, tissue temperature drops to  $-40^{\circ}\text{C}$  around needle tip, which is lethal for cells included in the iceball volume. The final goal of cryotherapy is the necrosis of cancerous cells while preserving surrounding healthy tissue and avoiding

damages to vital anatomical structures. For this purpose, an accurate surgical planning needs to be done beforehand by surgeons.

However, the non-invasive, real-time monitoring of three-dimensional isotherm surface of this critical temperature within the tissue during cryosurgical procedures has remained a challenge. Since temperature can be measured only at discrete points in the target region, simulation of heat transfer is an extremely useful tool to estimate the real coverage for a candidate probe placement. A number of models has been proposed to solve the bioheat propagation equation in two and three dimensions.

An important parameter in cryosurgery planning is the optimal choice of cryoprobes locations with specific shapes and dimensions. It is typically done in a trial-and-error task to find the best configuration. Since the manufactured cryoprobes have been produced with a limited set of active lengths and diameters, and freezing protocol is commonly fixed, other cryosurgical parameters such as number of cryoprobes and cryoprobe placement are good candidates for optimization and planning during the procedure.

The overall objective of our research is to provide the surgeon with an automatic pre-operative path planning algorithm able to propose a placement for multiple needles in 3D, taking into account several surgical constraints as well as a precise computation of the frozen area. In this paper, we focus on the optimization of the tridimensionnal placement of multiple iceballs around the tumor to cover it at best. We first explain the implementation of the accurate simulation of the propagation of cold within the tissues. This simulation being a time-consuming process, we compare several optimization approaches under different conditions, to find the most suitable in terms of compromise between speed and accuracy, to be able to propose to the surgeon a good positioning strategy in a reasonable time.

## 2 Context

### 2.1 Related works

The problem of cryosurgery optimization was first addressed by Keanini and Rubinsky [1] using simplex method. The heat transfer equation was solved for a 3D domain with finite-difference method. Authors optimized only the number of cryoprobes and their geometrical dimensions (diameter and active length), but optimization of other parameters, such as cryoprobe placement in the target tissue and their thermal protocol, seems to be more practical. They used an idealized model and geometry for urethral warmer, prostate, bladder and rectum. In 2001 Baissalov et al. [2] studied simultaneous optimization of cryoprobe placement and thermal simulation using a gradient descent algorithm called L-BFGS-B method. They described a 3D solution based on the cumulative 2D transverse planes, but the shown results were only for 2D state in a prostate model.

Tanaka and Rubin [3] used a mechanical based method to solve the problem of cryoprobe optimization in two phases. Phase I called bubble-packing starts with generating ellipsoidal

elements (or bubbles) inside planning domain, then van der Waals'-like forces are simulated to move these bubbles until a minimum-force configuration is found. A single bioheat simulation is executed at the end of Phase I. The simulation is terminated at the point at which a minimum defect region is found for that particular layout. In phase II, a bioheat equation is solved and a new set of forces on the cryoprobes are computed based on the defect region and one or more cryoprobes are moved accordingly. This survey was done in 2D for the prostate while in 2008, the same team extended their work to 3D [4] but just for bubble packing method.

Giovanni et al. [5] used Ants Colony (ACO) to choose the optimal parameter configurations. Computation of the cost function is based on the numerical solution of several direct Stefan problems solved by a Euler-Galerkin approach. This method combines a finite difference approximation of the time-derivative and a finite element approach solving the space-dependent part of the differential problem. This study was done on a 2D standard prostate phantom.

## 2.2 Problem statement

As mentioned above all previous studies were done for prostate cryosurgery in which needles are placed in the same direction and consequently number of optimization variables is reduced. In this paper the first goal is to deal with a general case in which planning domain could be 3D and needles have 6 degrees of freedom: 3 translations for position and 3 rotations for orientation.

Previous studies have computed bioheat propagation in order to have a more realistic simulation of cryosurgery procedure. Bioheat propagation in the tissue is affected by needle parameters, time and surrounding tissues. An interesting source of bioheat is the flowing blood within large adjacent vessels which can cause a "heat sink" effect and may prevent temperature from decreasing to lethal levels. This may result in inadequate ablation, thus increasing the risk of tumor recurrence in this region. Our second objective is to consider surrounding tissues which have an important role in forming the final frozen region inside the bioheat equation computation.

Our problem of simultaneous optimization of thermal protocol and cryoprobe placement requires handling a large number of bound constrained optimization variables and ability to minimize an objective function that cannot be expressed analytically in terms of the optimization variables.

High computational cost of bioheat equation in each iteration requires a fast converging optimization method for real time purposes. Optimization algorithms have been studied in the literature to find the most suitable ones in terms of convergence and computational time while avoiding local minima. Among the optimization techniques, we experimented various techniques in order to compare them in the conditions of our problem: local optimization methods such as Generating Set Search(GSS), and global optimization methods such as

Genetic Algorithm(GA), Simulated Annealing(SA), Multilevel Coordinate Search (MCS), Surrogate Modeling (SM) and evolutionary strategy (ES) were tested. Our final goal is to optimize trajectories positions quickly and precisely, while taking into account a realistic simulation of the formation of iceballs.

### 3 Material and Method

#### 3.1 Numerical computation of the bioheat transfer within the tissues

The thermal distribution outcome of the cryosurgical procedure is predicted using multi-probe thermal simulations. Results of the simulations are quantified in terms of isotherm locations at any given time with respect to anatomy and the value of the objective function in the optimization scheme. These tools provide a means of assessing effectiveness of the treatment. Our method consists of a time-dependent model of iceball formation based on bioheat transfer equation around the needle tip, taking into account major vessels surrounding the frozen area that influence the freezing process. Most of the theoretical analysis on heat transfer in living tissue are originated from the Pennes equation [6], which describes the influence of blood flow on the temperature distribution in the tissue in terms of volumetrically distributed heat sinks or sources.

This uniform energy equation for biological tissue which can be applied to frozen, partially frozen and unfrozen tissue regions, can be written as:

$$\tilde{C} \frac{\partial T(X, t)}{\partial t} = \nabla \cdot \tilde{k} \nabla [T(X, t)] - \tilde{\omega}_b C_b T(X, t) + \tilde{Q}_m + C_b \tilde{\omega}_b T_a \quad X \in \Omega(t) \quad (1)$$

where  $\tilde{C}$  is the effective heat capacity;  $\tilde{k}(T)$  is the effective thermal conductivity;  $\tilde{Q}_m$  is the effective metabolic heat generation;  $\tilde{\omega}_b(T)$  is the effective blood perfusion;  $T_a$  is the arterial temperature;  $C_b$  is the heat capacity of blood;  $X$  contains the Cartesian coordinates  $x$ ,  $y$ , and  $z$ ;  $T(X, t)$  is the temperature of tissue;  $\Omega(t)$  denotes the domain at time  $t$ . The description and derivation of this coefficients in different states are omitted here for brevity. A finite difference algorithm is applied to solve this complex problem with phase change heat transfer in biological tissues. Applying this formulation to Eq 1 and using the following relation to express the linear term  $T(X, t)$  on the right side of Eq 1,

$$T(X, t) = \beta T(X, t + \Delta t) + (1 - \beta) T(X, t) \quad (2)$$

where  $\beta$  is a relaxation factor, and  $0 \leq \beta \leq 1$ , Eq 1 can be discretized as follows:

$$\begin{aligned} T(X, t + \Delta t) = & \frac{1 - W(1 - \beta)\Delta t - m.Fo}{1 + W\beta\Delta t} T(X, t) + \sum_{i=1}^{\frac{m}{2}} \frac{Fo}{1 + W\beta\Delta t} T(X + \Delta x_i, t) \\ & + \sum_{i=1}^{\frac{m}{2}} \frac{Fo}{1 + W\beta\Delta t} T(X - \Delta x_i, t) + \frac{(\tilde{Q}_m + \tilde{\omega}_b C_b T_a)\Delta t}{1 + W\beta\Delta t} \end{aligned} \quad (3)$$

where  $\Delta t$  is the time increment;  $W = \tilde{\omega}_b C_b / \tilde{C}$ , and  $Fo = \tilde{k} \cdot \Delta t / \tilde{C} \cdot \Delta x^2$  is the Fourier number;  $m = 2, 4, 6$  correspond to the cases of one, two and three dimensions respectively, and in order to avoid numerical instability, the space and time steps are limited by  $1 - W(1 - \beta)\Delta t - m \cdot Fo \geq 0$ . Applying the boundary conditions at time  $t + \Delta t$  and substituting the calculated results at the previous time  $t$ , the unknown  $T$  at time  $t + \Delta t$  can be solved from the above equation.

The tissue domain is prescribed in a rectangular geometry with  $7 \times 7 \times 7$  cm in the  $x$ ,  $y$  and  $z$  directions respectively, in which  $x$  denotes the tissue depth from the skin surface while  $y$  and  $z$  are along the surface. The boundary conditions at the probe surface are prescribed respectively according to probe tip and probe shank as:  $T = -196^\circ\text{C}$  at probe tip;  $\partial T / \partial n = 0$  at probe shank. The initial temperature in tissue is simplified as  $T_0 = 37^\circ\text{C}$ . In calculations, the grid resolution is  $\Delta x = \Delta y = \Delta z = 1\text{mm}$  and  $\Delta t = 0.1\text{s}$ .  $\tilde{Q}_m = 0$  in a highly vascularized tissue like liver and  $\tilde{\omega}_b = 0.005$ .

Our routine is described as below:

1. The location of liver, tumor, skin and vessels are determined thanks to a segmentation process performed on the images. In this step, a 3D mesh for each anatomical structure are reconstructed. All vessels are considered as fixed sources of heat at  $37^\circ\text{C}$
2. The shape of needle tip has been designed to fit real cryoprobes
3. Needle tip is placed at an initial position and orientation inside the tumor manually or by the optimization method
4. The simulation procedure imitates a standard cryoablation pattern that consists of two 10 minutes freezing intervals and one 5 minutes thawing step in between, which is congruent with needle manufacturer calibration data in a tissue-like gel, which from now on we call reference data
5. The iceballs are obtained by a 3D reconstruction of the  $-40^\circ\text{C}$  isotherm surfaces. The selected value was chosen according to surgeons needs, as this temperature is used as a threshold to determine the resulting necrosis volume

### 3.2 Optimization of the probes placement in 3D

The optimization process allows to refine the number and placement of the needles (3 translations and 3 rotations for each) to minimize a defect function. It is based on an iterative procedure including the bioheat equation resolution at each step. Every resolution begins with the assumption that the placement of cryoprobes is given with a fixed tip temperature of  $-196^\circ\text{C}$  while the initial temperature of tumor and background tissue is  $37^\circ\text{C}$ . Then, the bioheat equation can be solved. The resulting temperature field is processed

to evaluate the defect function providing a quantitative estimate of the mismatch between the frozen tissue and the target tissue. Eq.4 shows the definition of the cost function.

More formally, a specific configuration of the cryosurgery design is represented by a state variable  $U$ , which is a list of  $N$  operating parameters (position of cryoprobes) whose admissible values are contained in  $S \subset R^N$ . The cost function is the defect weighting function  $F : S \rightarrow \mathbb{N}$  such that:

$$F(\theta_U) = \int_V \mu(\theta_U(x)) dx, \quad (4)$$

where  $\theta_U$  is the temperature distribution associated to  $U$  and

$$\mu(\theta(x)) = \begin{cases} 0 & \text{if } \theta(x) < \tilde{\theta} \text{ and } x \text{ is diseased,} \\ 1 & \text{if } \theta(x) < \tilde{\theta} \text{ and } x \text{ is healthy,} \\ 1 & \text{if } \theta(x) \geq \tilde{\theta} \text{ and } x \text{ is diseased,} \\ 0 & \text{if } \theta(x) \geq \tilde{\theta} \text{ and } x \text{ is healthy,} \end{cases} \quad (5)$$

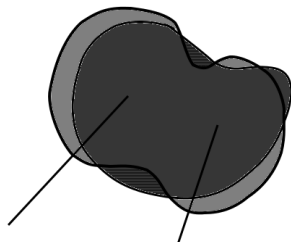


Figure 1: Schematic representation of the defect region. Tumor is in dark grey, and interacting iceballs is in light grey. Not damaged tumor parts are striped and damaged healthy tissue is in very light grey.

A schematic view of this function is demonstrated in Fig.1. Optimization algorithms use this objective function and yield the new positions of cryoprobes in order that the next step can begin. The procedure stops when further correction of the position of cryoprobes becomes negligible or the predefined maximum number of iterations is reached.

Conventional optimization techniques typically require multiple evaluations of the cost function for each iteration. For example, gradient based algorithms would require multiple function evaluations to compute the gradients [7]. Keanini and Rubinsky [1] stated that methods which compute explicit derivatives are likely to be inefficient. Our work employs techniques that avoid calculating derivatives so as to minimize the number of simulations.

As mentioned above our optimization algorithm should be capable of handling a large number of bound constrained optimization variables and be able to minimize an objective function that cannot be expressed analytically in terms of the optimization variables. Keeping these parameters in mind, a bound constrained derivative free optimization method which do not stuck in local minima (global optimization) with low number of iterations would be suitable. Our problem is a convex optimization problem because of cubic search domain surrounding the target region.

Derivative free optimization methods are classified to local and global optimization methods as well as as deterministic, model based and stochastic methods[8]. Six optimization methods were selected based on the parameters just mentioned in order to compare their strengths and weaknesses to our problem.

- Local methods:
  - Deterministic:
 

**Pattern search:** Generating Set Search (GSS) method was selected between different pattern search methods. Each iteration of GSS method consists of two basic steps. The search step is performed first over a finite set of search directions  $H_K$  generated by some, possibly heuristic, strategy that aims to improve the current iterate but may not guarantee convergence. If the search step fails to produce a better point, GSS method continues with the poll step, which is associated with a generating set that spans positively  $R^n$ . Generating sets are usually positive bases, with a cardinality between  $n+1$  to  $2n$  [9].
- Global methods:
  - Deterministic:
 

**Multilevel coordinate search (MCS):** It partitions the search space into boxes and in each iteration a label is assigned to each box based on the number of times it has been splitted. MCS selects boxes with the lowest objective value for each level value and marks them as candidates for splitting and will converge when the maximum number of s is reached [10].
  - Model based:
 

**Surrogate Modelling (SM):** Building a model of objective functions in our search domain allows us to optimize a function with less number of iterations. In order to build such a model, one should starts with sampling the search domain and construct an initial surrogate model. Then optimizers are used to converge the model, evaluate the best point and update the surrogate model. For this purpose we have employed a mixture of radial basis functions [11] and kriging [12] interpolations for our surrogate model. Radial basis functions approximate

f by considering an interpolating model based on radial functions and kriging models a deterministic response as the realization of a stochastic process by means of a kriging basis function.

– Stochastic:

**Simulated Annealing (SA):** At iteration  $k$ , simulated annealing generates a new trial point  $\hat{x}$  that is compared to the incumbent  $x^k$  and accepted with a probability function [13].

$$P(\hat{x}|x_k) = \begin{cases} \exp\left[\frac{f(\hat{x})-f(x_k)}{T_k}\right] & \text{if } f(\hat{x}) < f(x_k) \\ 1 & \text{if } f(\hat{x}) \geq f(x_k) \end{cases} \quad (6)$$

**Genetic algorithms (GA):** This method introduced by Holland [14] resembles natural selection and reproduction processes governed by rules that assure the survival of the fittest in large populations. Individuals (points) are associated with identity genes that define a fitness measure (objective function value). A set of individuals form a population, which adapts and mutates following probabilistic rules that utilize the fitness function.

**Evolution Strategies (ES):** This method belongs to the class of Evolutionary Algorithms (EAs) which use mutation, recombination, and selection applied to a population of individuals containing candidate solutions in order to evolve iteratively better and better solutions.

### 3.3 Experiment design

Our experiments were done on two patient models from the 3D-IRCADb database. They are reconstructed images of liver tumors surrounded by vessels and normal liver tissue. To test different conditions, we chose a case with a small tumor and another with a large one.

For the tests we experimented several parameters, each time changing one parameter while others were fixed. Optimization methods, number of needles and size of the tumors were selected as different experimental designs. Six optimization methods were considered as mentioned in the previous section. In order to compute defect volume, the bioheat equation was solved in each iteration and then objective function value was computed by comparing temperature of each point in the tissue domain.

Comparisons for speed and convergence of the optimization methods are based on the solution profile of each optimizer for few iterations to large ones. We tried to check the sensitivity of each optimizer to other parameters like tumor size and number of electrodes. Tumor size will affect complexity of the problem by extending or shrinking the search domain and number of needles will modify the optimization input variables. In order to have a fair comparison, four different experimental designs are selected, two for small tumor and two

for large ones. In each state there are two possibilities of choosing 3 or 5 needles. All solvers had a maximum of 500 iterations.

The type of cryoprobe we modeled was a PERC-24 from Endocare. The theoretical volume of iceball ( $-40^{\circ}\text{C}$  isotherm surface) of this cryoprobe type, given by the manufacturer, is  $2.4 \times 2.4 \times 4 \text{cm}$ . Ratio between theoretical single iceball volume and tumor volume allows to select the right initial number of needles. We experimented our optimizations on two tumor sizes, small and large. This ratio is 0.7 for small and 0.2 for large tumor, with the chosen cryoprobe type. In order to destroy tumors, it is intuitive to start with a number of needles providing a total iceballs volume at least equal to the tumor volume.

## 4 Results and discussion

An example of the computation of an iceball produced by 3 needles around the small tumor is shown on Fig.2. Fig.3 shows the trends of defect volume versus iteration number in different conditions: small / large tumors and 3 / 5 needles. Optimization time lapse is directly related to the number of iterations for all optimizers except surrogate modeling. The most time consuming part of optimization process is the solution of bioheat equation which is computed once per iteration. It takes 5 seconds with spatial dimensions mentioned above on a machine using Intel core i7 3.4 to simulate a 10 minutes cryoablation treatment.

Covering the whole tumor with a minimum number of needles demands a lot of iterations for the optimizer to reach a global minimum. Moreover, adding extra needles will increase the number of optimization variables and consequently the risks of increasing healthy tissue region which is damaged, but an optimum number of needles for any size of tumor should be found. This trend is visible in the results shown in Fig.3 top for a small tumor in which the total percentage of defect volume increased by growing the number of needles. Also in Fig.3 bottom, total defect volume for a large tumor decreased by an increase in number

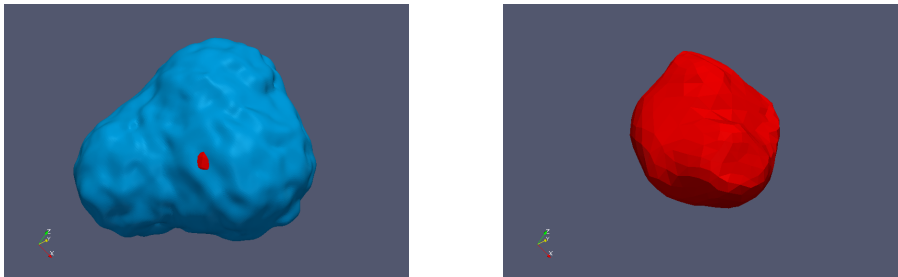


Figure 2: Example of aggregated iceball (left) after a heat propagation simulation for the small tumor (right) and 3 needles. This configuration is not completely optimal as a part of the tumor is outside the iceball.

## MULTI PROBE OPTIMIZATION FOR LIVER CRYOSURGERY

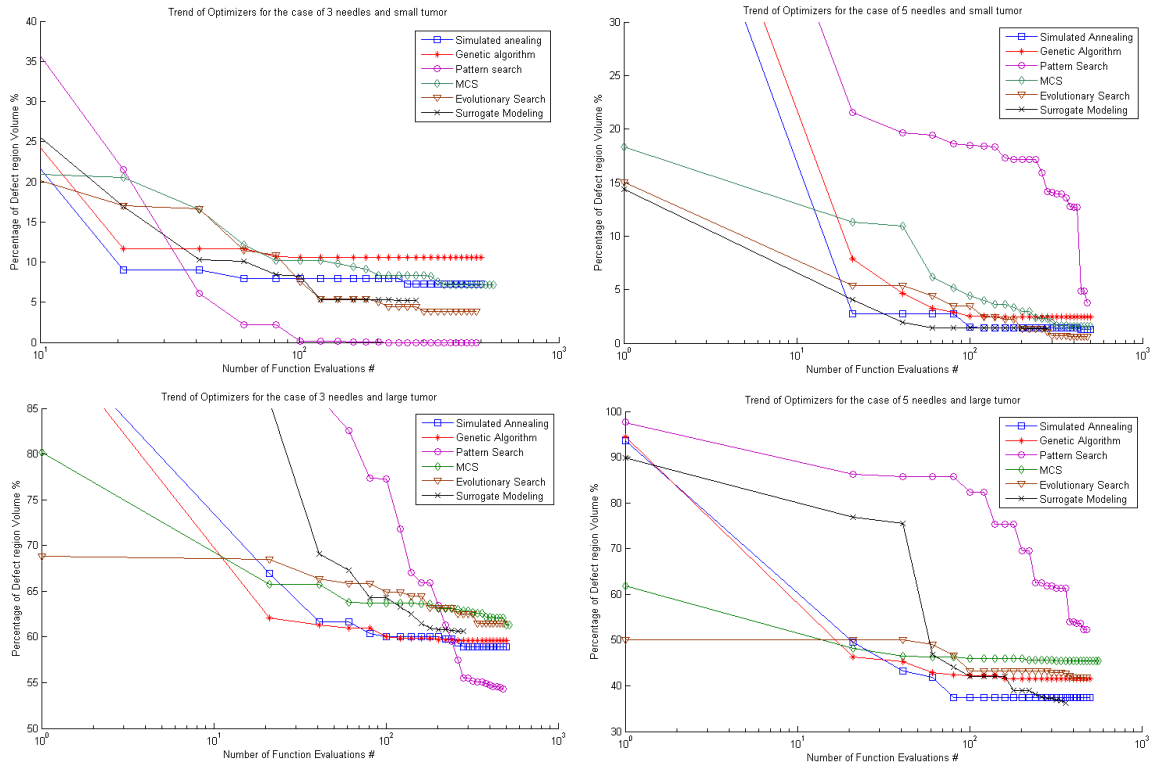


Figure 3: Trend of 6 optimizers for the case of small (top) and large (bottom) tumor are shown above for 3 and 5 needles. Vertical axis shows percentage of defect volume while horizontal axis shows number of iteration for a maximum of 500 iterations

of cryoprobes. Due to the low ratio of iceball volume to tumor volume and large size of the tumor, even with 5 needles we did not find a global minimum within 500 iterations. Increasing number of iterations or number of needles seems to be the first intuitive solutions but due to the computational time for bioheat equation we did not consider them, pursuing our goal to integrate selected methods in our existing planning tool which should converge in the order of minutes for real-time applications.

In speed comparison of each experimental design we are interested to see which method had the minimum of defect volume in its first one hundred iterations. By choosing this criteria and looking into Fig.3 top left graph, GSS local method is prior to others. In this design, thanks to large ratio of iceball volume to tumor volume and less low number of needles, we are facing a simple problem which can be solved easily by a local deterministic solver. Other solvers had more or less the same speed in this scenario. On the right graph, by increasing tumor size both deterministic methods decrease their performance especially

for the GSS method but for other solvers speed of optimization was not affected by changing the search domain. The same characteristic is shown in Fig.3 bottom for large tumor.

For the accuracy comparison we looked for the method which finds the lowest defect volume regardless of number of iterations. In general evolutionary methods had better flexibility than heuristic methods like MCS and GSS. Simulated annealing did rapid convergence among global methods but it is dependent on its initial point therefore the results are not always good with different initial point and tumor shapes. MCS had more or less good results in long iterations regardless of problem complexity due to its global design. SM had the same performance of speed and accuracy comparing to simulated annealing but it was more robust due to changing conditions and tumor shapes. Surrogate modeling also demonstrated better results for complex problems as Fig.3 on the right which is the most complicated among our designs. The strength of this approach lies in the generality of its formulation since SM is independent of the physical interpretation and from the number of the parameters subjected to optimization. In other words, through SM, one is able to set different kinds of free planning parameters without changing the optimization technique.

## 5 Conclusion and future works

In this study, we compared six derivative free optimization methods. The speed and accuracy of each method was investigated due to number of needles and tumor size. Generating Set Search was selected as fastest for simple problems and Surrogate Modeling as the most robust in complex ones. We have demonstrated our tests by solving bioheat equation inside the optimization process for a 3D cryosurgical planning of two tumor sets of small and large size. Objective function was defined based on the defect volume value and did not consider its shape. We believe that taking into account the shape of objective function will lead to higher precision and lower number of iterations in future works. In order to solve the mentioned convergence problem for large tumors in an acceptable time we are thinking about experimenting smarter routines like supervised methods or multi stage optimization.

## Acknowledgments

Authors would like to thank CNRS and Region Alsace for funding this work.

## References

- [1] Keanini, R., Rubinsky, B.: Optimization of multiprobe cryosurgery. *Heat Transfer* **114**(4) (1992) 796–801

- [2] Baissalov, R., Sandison, G., Reynolds, D., Muldrew, K.: Simultaneous optimization of cryoprobe placement and thermal protocol for cryosurgery. *Physics in medicine and biology* **46**(7) (2001) 1799
- [3] Tanaka, D., Shimada, K., Rabin, Y.: Two-phase computerized planning of cryosurgery using bubble-packing and force-field analogy. *Journal of biomechanical engineering* **128**(1) (2006) 49
- [4] Tanaka, D., Shimada, K., Rossi, M.R., Rabin, Y.: Cryosurgery planning using bubble packing in 3d. *Computer methods in biomechanics and biomedical engineering* **11**(2) (2008) 113–121
- [5] Giorgi, G., Avalle, L., Brignone, M., Piana, M., Caviglia, G.: An optimisation approach to multiprobe cryosurgery planning. *Computer Methods in Biomechanics and Biomedical Engineering* (ahead-of-print) (2011) 1–11
- [6] Pennes, H.H.: Analysis of tissue and arterial blood temperatures in the resting human forearm. *Journal of applied physiology* **1**(2) (1948) 93–122
- [7] Vanderplaats, G.N.: Numerical optimization techniques for engineering design: with applications. Volume 32. McGraw-Hill New York (1984)
- [8] Rios, L.M., Sahinidis, N.V.: Derivative-free optimization: A review of algorithms and comparison of software implementations. *Journal of Global Optimization* (2012) 1–47
- [9] Kolda, T.G., Lewis, R.M., Torczon, V.: Optimization by direct search: New perspectives on some classical and modern methods. *SIAM review* **45**(3) (2003) 385–482
- [10] Huyer, W., Neumaier, A.: Global optimization by multilevel coordinate search. *Journal of Global Optimization* **14**(4) (1999) 331–355
- [11] Powell, M.J.: Recent research at Cambridge on radial basis functions. Springer (1999)
- [12] Sacks, J., Welch, W.J., Mitchell, T.J., Wynn, H.P.: Design and analysis of computer experiments. *Statistical science* **4**(4) (1989) 409–423
- [13] Powell, M.J.: Uobyqa: unconstrained optimization by quadratic approximation. *Mathematical Programming* **92**(3) (2002) 555–582
- [14] Holland, J.H.: Adaptation in natural and artificial systems: An introductory analysis with applications to biology, control, and artificial intelligence. U Michigan Press (1975)